

UNCLASSIFIED

AD NUMBER
ADB005619
NEW LIMITATION CHANGE
TO Approved for public release, distribution unlimited
FROM Distribution authorized to U.S. Gov't. agencies and their contractors; Critical Technology; JUL 1975. Other requests shall be referred to Director, U.S. Army Ballistic Research Labs., Attn: AMXBR-SS, Aberdeen Proving Ground, MD 21005.
AUTHORITY
USAARDC ltr dtd 8 Mar 1978

THIS PAGE IS UNCLASSIFIED

THIS REPORT HAS BEEN DELIMITED
AND CLEARED FOR PUBLIC RELEASE
UNDER DOD DIRECTIVE 5200.20 AND
NO RESTRICTIONS ARE IMPOSED UPON
ITS USE AND DISCLOSURE.

DISTRIBUTION STATEMENT A

APPROVED FOR PUBLIC RELEASE;
DISTRIBUTION UNLIMITED.

BRL MIR 2496

BRL

AD

MEMORANDUM REPORT NO. 2496

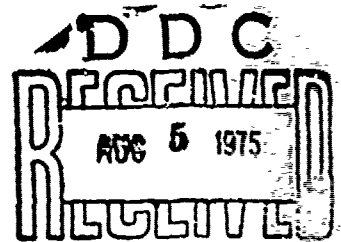
EXPERIMENTS ON WAKE OPTICAL PROPERTIES

AD B 005619

George D. Kahl
David B. Sleator
Donald D. Shear

July 1975

Distribution limited to US Government agencies only; Test and Evaluation; J. 1, 7. Other requests for this document must be referred to Director, USA Ballistic Research Laboratories, ATTN: AMXBR-SS, Aberdeen Proving Ground, Maryland 21005.



A

USA BALLISTIC RESEARCH LABORATORIES
ABERDEEN PROVING GROUND, MARYLAND

Destroy this report when it is no longer needed.
Do not return it to the originator.

Secondary distribution of this report by originating
or sponsoring activity is prohibited.

Additional copies of this report may be obtained
from the Defense Documentation Center, Cameron
Station, Alexandria, Virginia 22314.

The findings in this report are not to be construed as
an official Department of the Army position, unless
so designated by other authorized documents.

UNCLASSIFIED

SECURITY CLASSIFICATION OF THIS PAGE (When Data Entered)

REPORT DOCUMENTATION PAGE		READ INSTRUCTIONS BEFORE COMPLETING FORM
1. REPORT NUMBER BRL Memorandum Report No. 2496	2. GOVT ACCESSION NO.	3. RECIPIENT'S CATALOG NUMBER
4. TITLE (and Subtitle) EXPERIMENTS ON WAKE OPTICAL PROPERTIES		5. TYPE OF REPORT & PERIOD COVERED Final
		6. PERFORMING ORG. REPORT NUMBER
7. AUTHOR(s) George D. Kahl, David B. Sleator, and Donald D. Shear		8. CONTRACT OR GRANT NUMBER(s)
9. PERFORMING ORGANIZATION NAME AND ADDRESS USA Ballistic Research Laboratories Aberdeen Proving Ground, Maryland 21005		10. PROGRAM ELEMENT, PROJECT, TASK AREA & WORK UNIT NUMBERS RDT&E 1T161102A33D
11. CONTROLLING OFFICE NAME AND ADDRESS U.S. Army Materiel Command 5001 Eisenhower Avenue Alexandria, Virginia 22333		12. REPORT DATE JULY 1975
		13. NUMBER OF PAGES 29
14. MONITORING AGENCY NAME & ADDRESS (if different from Controlling Office)		15. SECURITY CLASS. (of this report) UNCLASSIFIED
		15a. DECLASSIFICATION/DOWNGRADING SCHEDULE
16. DISTRIBUTION STATEMENT (of this Report) Distribution limited to US Government agencies only; Test and Evaluation; July 1975. Other requests for this document must be referred to Director, USA Ballistic Research Laboratories, ATTN: AMXBR-SS, Aberdeen Proving Ground, MD 21005.		
17. DISTRIBUTION STATEMENT (of the abstract entered in Block 20, if different from Report)		
18. SUPPLEMENTARY NOTES		
19. KEY WORDS (Continue on reverse side if necessary and identify by block number) Wake Optical Deviation Projectile Wakes Wake Optics Refraction in Wakes Miss-Distance Indicator Wakes		
20. ABSTRACT (Continue on reverse side if necessary and identify by block number) (ner) A simple experimental test was done to examine the optical effect of a light beam sent up the wake of a projectile. The results show that the wake acts as a diverging lens to this light beam. Measurements of the optical deviation were made. Some consequences of this effect on certain miss-distance in- dicators are discussed.		

TABLE OF CONTENTS

	<u>Page</u>
LIST OF ILLUSTRATIONS	5
I. INTRODUCTION	7
II. EXPERIMENTAL PROCEDURE	7
III. RESULTS	8
IV. CONCLUSIONS	10
V. APPLICATION TO MISS-DISTANCE SENSOR	10
APPENDIX A	21
DISTRIBUTION LIST	25

LIST OF ILLUSTRATIONS

<u>Figure</u>		<u>Page</u>
1.	Shadowgraph of the Near Wake From a Conventional Diameter Projectile, Mach 2.7	13
2.	Arrangement of Films and Light Source for Taking End View Shadowgraphs	14
3.	Typical End-View Shadowgraph of 30 Caliber Projectile 9.4 Inches From Film	15
4.	End-View Shadowgraphs of Fired and Statically-Mounted Projectiles	16
5.	Projectile Image Magnification Plotted Against Stand-off Distance, and Also Geometrical Magnification	17
6.	Angular Deviation From Grid Distortion. Grid, Projectile Base 16" and 4.5" From Film, Respectively. Grid Spacing Approximately 1/4 Inch; Deviation Always Away From Trajectory, Located at Grid $i = 5\frac{1}{2}$, $j = 6$	18
7.	Reconstruction of Finite Fringe Hologram, Showing Projectile, Shock Waves and Wake.	19

I. INTRODUCTION

The near wake behind a projectile, as shown in Fig. 1, is a tube-like region of disturbed gas located on the trajectory, and having an average diameter nearly that of the projectile. Although reasonably symmetric near the projectile, the wake structure further back shows an irregular edge, with protruding turbulent eddies. The mean wake diameter grows slowly with distance from the projectile, at about the one-third power¹; for example, at a distance of 1300 calibers, the diameter of the wake from a sphere was measured to be only 13 times that of the sphere.²

From the geometry of the wake, it is obvious that any method of optical communication with a sensor on the projectile base requires that light rays traverse some portion of the wake. If the ground station light transmitter is close to the trajectory, nearly all the light path of communication could be engulfed by the wake. Figure 1 demonstrates that light can be sent transversely through the wake, where the in-wake light path is only 3.0 cm. But information is needed about the effects of attenuation, scattering, and refraction on light rays traveling lengthwise up the wake for long distances, to assist in the design of optical sensing systems. Since such explicit information could not readily be found, a simple experiment was designed to probe these problems. The tests showed conclusively that the wake acts optically as a diverging lens for light rays traveling nearly lengthwise through it.

II. EXPERIMENTAL PROCEDURE

One part of the experiment consisted of taking nearly end-on shadowgraphs of the wake and projectile, using a pulsed light source located behind the projectile, very close to the trajectory. The configuration is shown schematically in Fig. 2. A caliber .30 projectile (diameter, 7.82mm) was fired toward a photographic film oriented normal to the trajectory. A small turning mirror located near the trajectory reflected a pulsed, diverging beam of laser light (wavelength, 6943 Å) toward the projectile at a predetermined time. This short-

1. C. H. Murphy and E. R. Dickinson, "Growth of the Turbulent Wake Behind a Supersonic Sphere," *AIAA Journal* **1**, 339-342, 1963. Also see BRL Memorandum Report 1388. AD 280216.
2. W. F. Fraun, "Growth of the Turbulent Inner Wake Behind Large Spheres at Supersonic Velocities," BRL Memorandum Report 1597, September 1964. AD 453850.

duration pulse (less than 100 nanosecs.) imprinted a shadow image on the film before the projectile pierced it. Since the virtual image of the effective point source was offset 4.5 cm from the trajectory, the projectile shadow was also centered off the trajectory; therefore, the subsequent piercing hole in the film did not completely obscure the shadow image.

The distance from the point source to the normal film, L , was 505 cm for six tests, and 204 cm for two tests. The stand-off distance, d , the distance between the normal film and the projectile base when the light was pulsed, ranged from 10 to 58 cm. In order to measure the projectile location when the shadowgraph was made, an additional turning mirror was placed alongside the trajectory to reflect part of the same light on a film oriented parallel to the flight path. An example of the end-on shadowgraph for $d = 24$ cm, $L = 505$ cm is shown in Fig. 3. In calibers, the wake lengths traversed by the light rays for these tests ranged from 246 to 632 calibers. Projectile velocity was 2900 feet/second.

III. RESULTS

The projectile shadowgraphs were measured and compared to the sizes expected from geometrical projection; the latter are easily computed from L and d , assuming small angles between the grazing light rays and the trajectory. But in every test the shadow with the wake was significantly larger than that computed from geometrical projection. An example is shown in Fig. 4, where the shadow of a projectile mounted in still air (geometric projection) is compared to that obtained with wake, each having the same distances $d = 23$ cm, and $L = 505$ cm; the shadow diameter with wake is 50% larger than the geometric projection. A graph of the measured magnifications with wake, M_w , as a function of stand-off distance is compared to the expected geometrical magnification, M_g , in Fig. 5.

The enlargement of the shadow caused by the wake gives a measure of the refractive deviation contributed by the wake to light rays which graze the outline of the base. The amount of deviation angle, $\Delta\psi$, can be estimated from

$$\Delta\psi \approx r (M_w - M_g)/d,$$

where r is the radius of the projectile; here again small angles are assumed between the grazing rays and the trajectory. Table I summarizes the results in terms of d and L . Excluding the last tabulated value, the average refractive deviation angle of these grazing rays is 3.6 milliradians.

This shadow method yields data about the refractive deviation of rays grazing the base, but gives none concerning inner rays incident

on the base, or outer rays missing the projectile. To help in assessing the wake effect on the outer rays, a screen grid of spacing 6.35mm was placed 40 cm ahead of the normal film, and a hole was cut to permit unhindered passage of the projectile. A pair of shadowgraphs of the screen was taken, one a control (still air) and one with a projectile wake $d = 11.5$ cm. The apparent displacements of the grid lines caused by the wake (in directions normal to the grid lines only) were measured and expressed in terms of refractive deviation angle using the 40 cm length from screen to film. Results of this test are shown in Fig. 6. The deviation was always away from the trajectory, which was located at grid $i = 5\frac{1}{2}$, $j = 6$. The point light source, if projected parallel to the trajectory, would fall on the grid point $i = 9.5$, $j = 12.4$. By comparing the grid line $i = 7$ with a straight edge, the reader can verify the outward bulging between $j = 4$ and 6; with no wake, this grid line is straight. The stub ends of the screen grid where the hole was initially cut also appear bent, but this was caused by the cutting process, and not by the wake.

This distortion of the screen grid projection by the wake shows that light rays traveling longitudinally through the outer wake radius are also deviated radially outward from the trajectory.

The method of measuring the shadow diameters deserves some mention. Readings from the films were made on a calibrated projection screen using 4 X magnification. In many instances the projectile shadowgraphs were outlined with diffraction fringes, as in Fig. 4, which made it difficult to determine the diameter of the effective geometrical shadow. The problem was solved by measuring the diameter of the first minima in terms of spacing of the first and second fringe minima, and applying a two-dimensional diffraction correction to the former. This method was independently checked on the no-flow test and appeared to work very well. From the Cornu function for diffraction by a straight edge³, the ratio of the distance between the ideal geometric projection of the projectile radius and the first fringe minimum compared to the spacing between the first two fringe minima was found to be 2.15.

The laser system employed was also used to reconstruct a holographic interferogram of the wake of this projectile, Fig. 7. Qualitatively, the fringe displacements in the wake indicate a smaller refractive index in the wake. This fact may be verified by comparing the "forward" fringe shifts inside the outer shock, with those "backward" shifts in the wake; the refractive index is known to be higher inside the outer shock.

3. F. T. Jenkins and H. E. White, Fundamentals of Physical Optics McGraw-Hill Book Co., New York, 1937 (pp. 188-195)

IV CONCLUSIONS

Light traveling nearly longitudinally up 600 calibers of wake toward the base of a projectile was found to retain enough coherence to outline clearly the shadow of this projectile (see Figure 4). This fact suggests that the expected turbulent fluctuations in the wake are not dominant in scattering and diffusing the light traveling the above distances up the wake.

Because the shadow of the projectile formed by this light is magnified, we conclude that the wake acts as a diverging (negative) lens on light traveling along the trajectory of the projectile. Since the divergence of the light was found to be the same for wake lengths of 250 and 630 calibers, we also conclude that the major cause of the spreading of the rays must be in the near wake, less than 250 calibers behind the projectile.

The deviation of the light was radially outward away from the trajectory. It was strongest for the light rays in the cone grazing the projectile ($\Delta\psi \sim 3.6$ millirads), and was much smaller for outer rays as measured by the grid distortion.

V. APPLICATION TO MISS-DISTANCE SENSOR

Light rays traveling up the wakes of projectiles have been demonstrated to be deviated radially outward; the wake acts optically as a variable strength diverging lens, causing some incident intensity loss. If the light rays are reflected from the projectile base back to some sensor, they then traverse the wake twice. A plane mirror on the projectile base to reflect those rays is impractical because it would be too sensitive to projectile yaw. Use of a single corner-prism mirror removes the yaw sensitivity, but aggravates the problem of the radial divergence effect of the wake.

The reason for this is that although the ideal corner mirror reflects an incident light ray by exactly 180° , the reflected ray is displaced symmetrically across the axis of the corner prism, due to the triple reflections. If the corner is centered on the projectile base, the incident deviated light ray would be reflected back, including the deviation angle, starting from a radial location symmetrically across the wake from the point of incidence. But because the wake optical effect is symmetric about the trajectory center line, an additional outward radial deviation would be given this reflected ray. Thus, the diverging effect of the wake is enhanced by a single corner prism reflector centered on the projectile base. One solution to help cure this might be to use a grid of very small corner prisms, so that the reflected ray, including deviation, is reflected back starting from nearly the same radial position with respect to

the wake as the incident ray. Then the wake deviation should be nearly cancelled, because of the reversibility property of ray optics.

To illustrate the importance of this problem for a single corner prism, we note that rays grazing the outside of the projectile base in these tests are deviated outward by about .0036 radians. Neglecting any additional deviation of the reflected ray back down the wake, these rays defining the outline of the projectile base, when projected back to the plane of the light source, give a greatly enlarged image of the base outline, due to their deviation. If the projectile were 1000 meters from the transceiver, the reflected rays defining the projectile outline in the plane of the transceiver would be circular, with a radius of 3.6 meters. This fact suggests considerable intensity loss on any reasonable size sensor, due to optical wake deviation.

These findings indicate that some additional investigations of wake optical properties, including a theoretical model, would be highly desirable for design concepts for optically communicating with projectiles.

TABLE 1. SUMMARY OF SHADOWGRAPH EXPERIMENTS

L(in)	d(in)	Mw	Mg	$\Delta\psi$ (rads)
80	4.15	1.140	1.054	.00319
80	4.67	1.175	1.062	.00399
199	4.52	1.150	1.023	.00433
199	8.11	1.230	1.042	.00357
199	9.39	1.260	1.050	.00344
199	16.27	1.410	1.089	.00504
199	23.15	1.640	1.132	.00338
199	28.00*	1.630	1.163	.00257

*No cross picture; estimated from delay set.



Figure 1. Shadowgraph of the Near Wake From a Conventional 30mm:
Diameter Projectile, Mach 2.7. Courtesy of W. Braun, USABRL

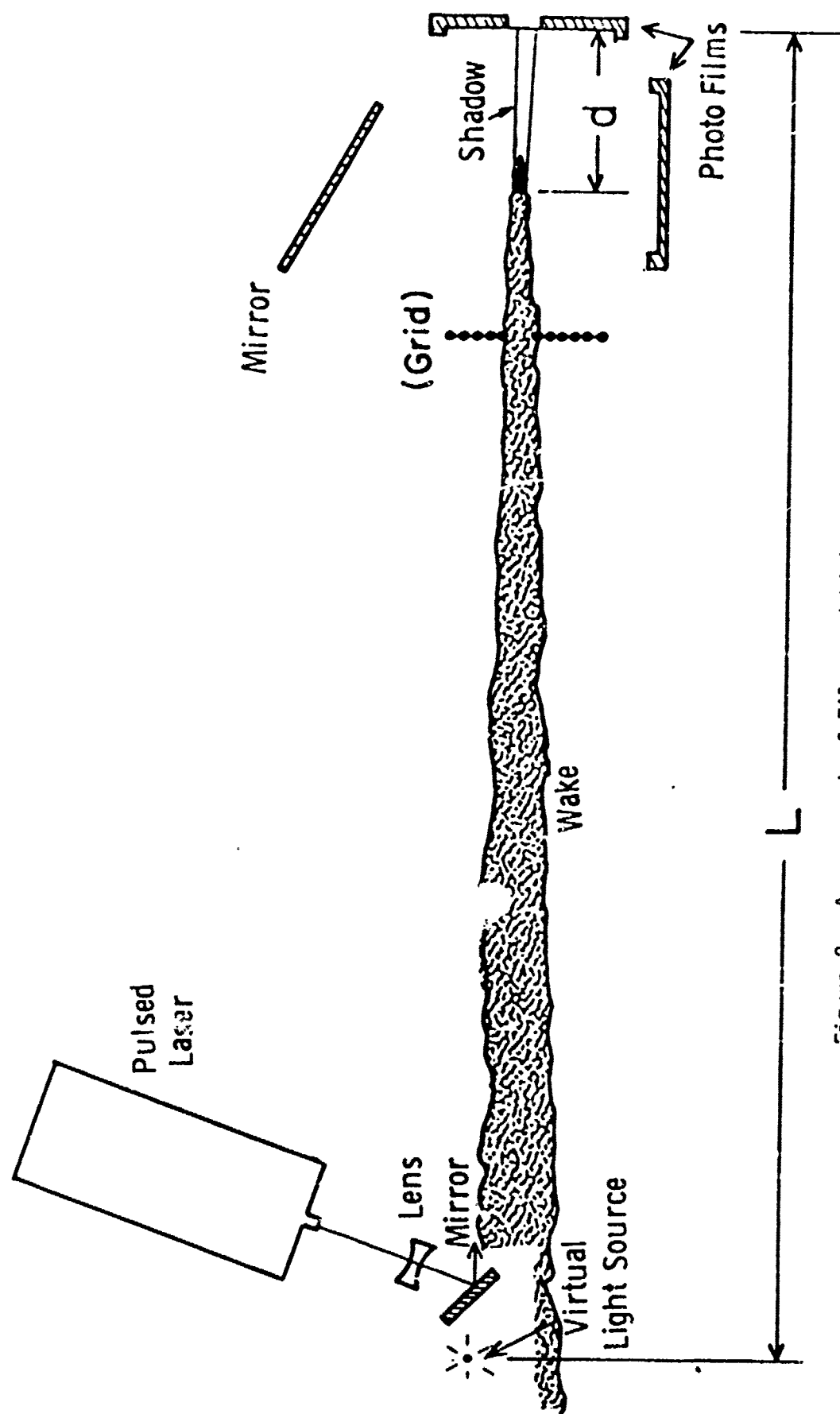


Figure 2. Arrangement of Films and Light Source for Taking End View Shadowgraphs



Figure 3. Typical End-View Shadowgraph of 30 Caliber Projectile 9.4 Inches from Film.

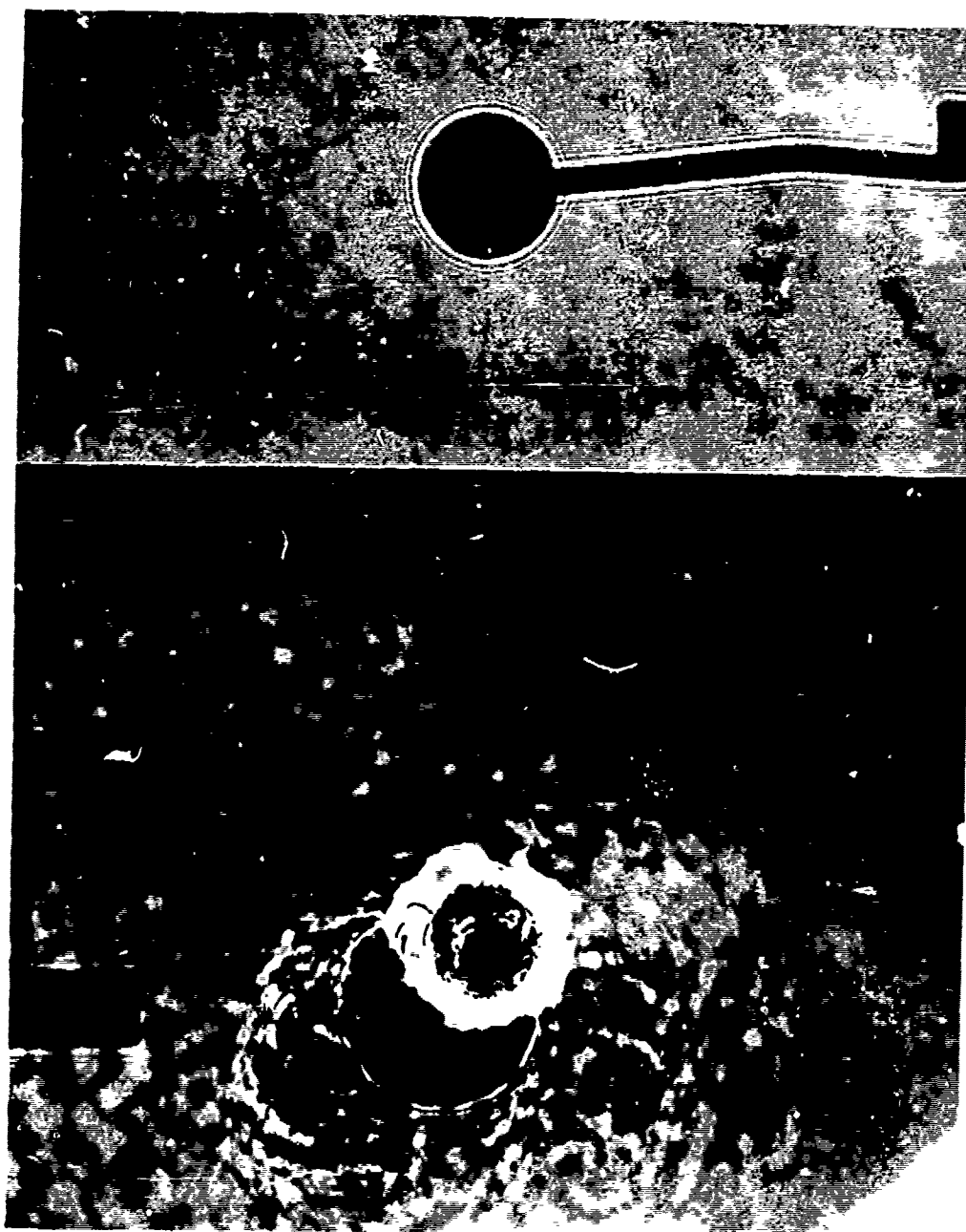
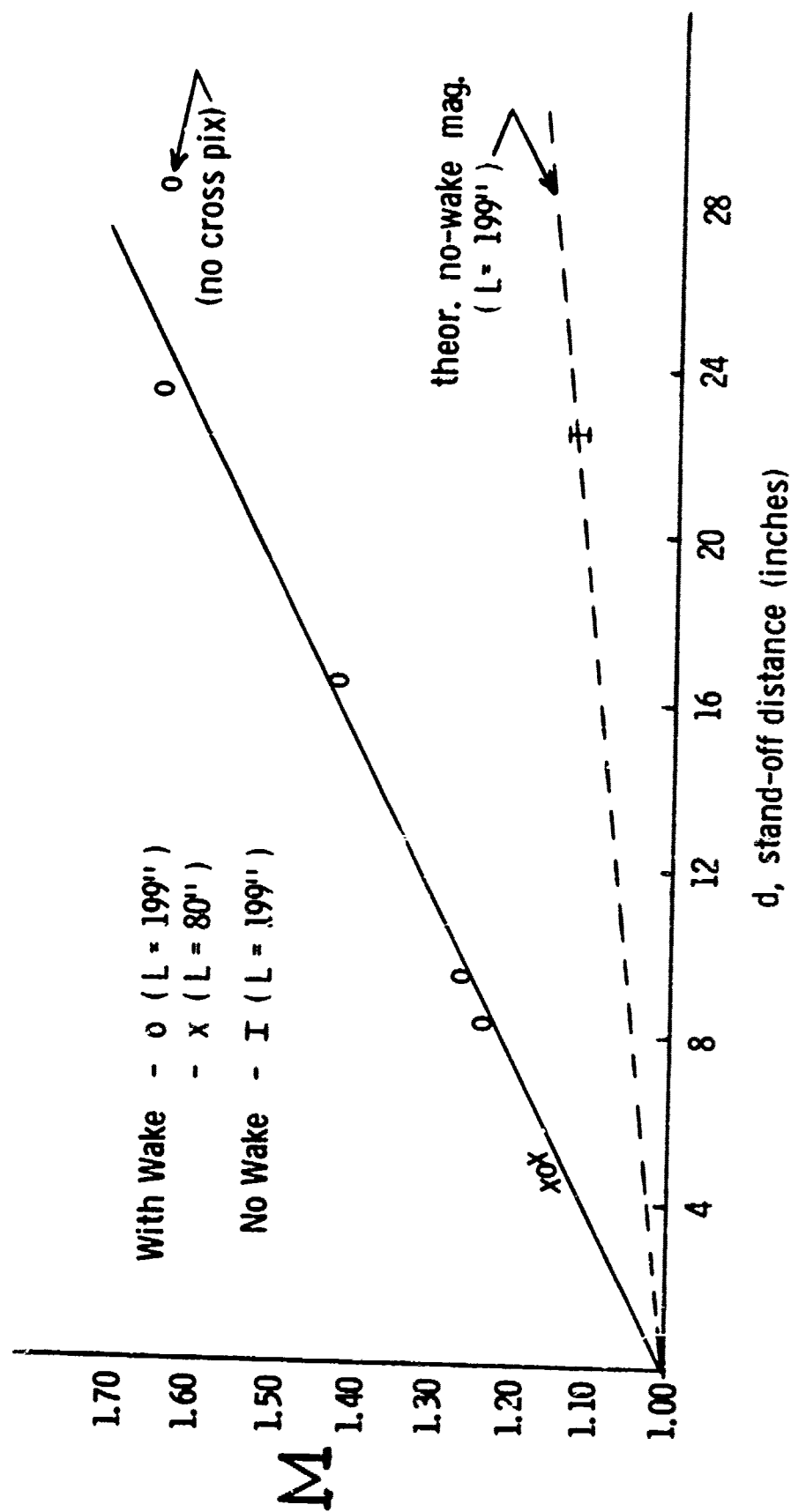


Figure 4. End-View Shadowgraphs of Fired and Statically-Mounted Projectiles



SHADOW MAGNIFICATION BY WAKES

Figure 5. Projectile Image Magnification Plotted Against Stand-off Distance, and Also Geometrical Magnification.

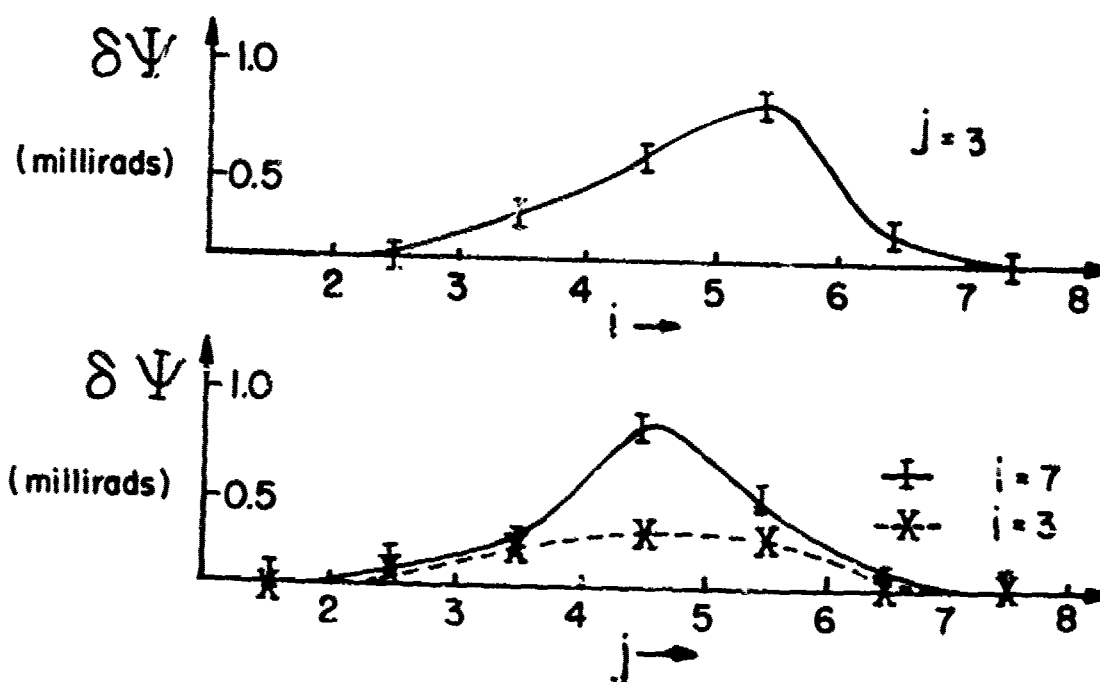
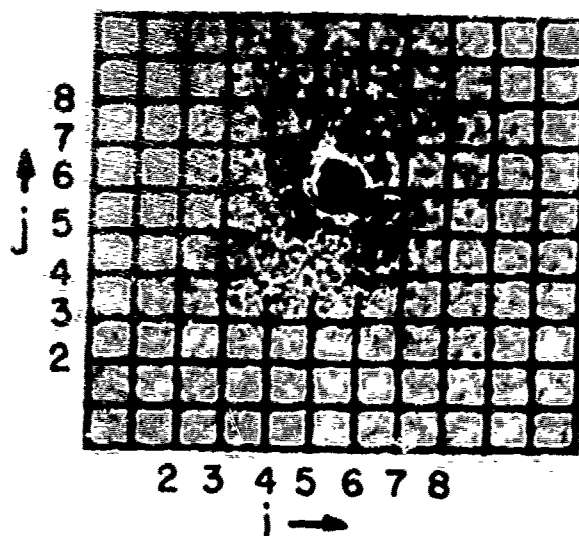


Figure 6. Angular Deviation From Grid Distortion. Grid, Projectile Base 16" and 4.5" From Film, Respectively. Grid Spacing Approximately 1/4 Inch; Deviation Always Away From Trajectory, Located at Grid $i = 5\frac{1}{2}$, $j = 6$.

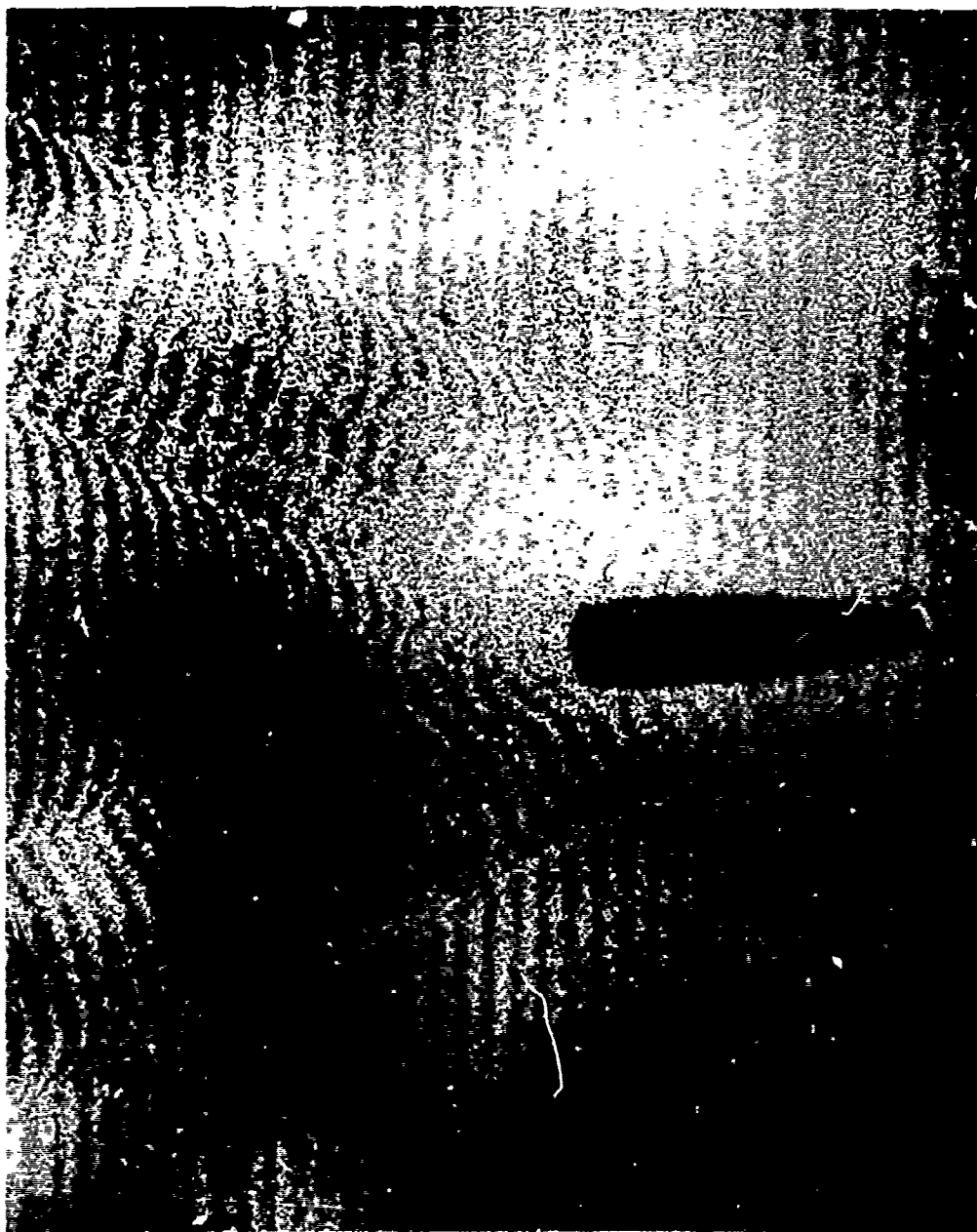


Figure 7. Reconstruction of Finite Fringe Hologram,
Showing Projectile, Shock Waves and Wake.

APPENDIX A: IDEAL CORNER REFLECTOR

A short analysis of the ideal corner reflector is given here to demonstrate that an incoming ray, after the triple reflection, is reversed exactly in direction and is displaced an equal and opposite distance across a centerline which is both parallel to the incoming ray and passes through the corner of the reflector.

Let the mirrors of the corner reflector be characterized by the unit, orthogonal, right-hand, vector triad $(\bar{i}, \bar{j}, \bar{k})$, so that the unit vectors are the outward normals to the respective mirror surfaces. Snell's reflection law from a plane mirror with outward unit normal \bar{n} is:

$$\bar{r}_r = \bar{r}_i \cdot \bar{\bar{R}}_n = \bar{r}_i \cdot (\bar{I} - 2\bar{n}\bar{n})$$

where \bar{r}_i and \bar{r}_r are unit vectors representing the incident and reflected light rays, respectively, $\bar{\bar{R}}_n$ is the plane reflection dyadic defined above, with \bar{I} the identity dyad, equal to $\bar{i}\bar{i} + \bar{j}\bar{j} + \bar{k}\bar{k}$. Note also that $\bar{r}_i = \bar{r}_r \cdot \bar{\bar{R}}_n$. Multiple reflections are treated by letting the subsequent incident ray be the same as the previous reflected ray. Therefore, in the notation above, the final outgoing ray \bar{r}_f after a triple reflection of an incident ray \bar{r}_c from mirrors $\bar{i}, \bar{j}, \bar{k}$ can be expressed by

$$\bar{r}_f = \bar{r}_c \cdot (\bar{\bar{R}}_i \cdot \bar{\bar{R}}_j \cdot \bar{\bar{R}}_k)$$

However, $(\bar{\bar{R}}_i \cdot \bar{\bar{R}}_j \cdot \bar{\bar{R}}_k) = -\bar{I}$ using the above orthogonality conditions. Moreover, the order of the reflections does not alter this result; therefore, $\bar{r}_f = -\bar{r}_c$, and the outgoing ray is exactly reversed in direction from the incoming ray.

The location of the points of contact on the corner reflector of the incoming and outgoing rays in terms of the corner must still be found. Assume that the incident ray, \bar{r}_c is equal to $-\bar{c}$, where \bar{c} is a unit vector from the corner, given by

$$\bar{c} = u\bar{i} + v\bar{j} + w\bar{k},$$

where

$$0 < u, v, w < 1,$$

and consider the triple reflection that occurs sequentially from the \bar{i} to \bar{j} to \bar{k} mirrors. Let the points of contact on the \bar{i} , \bar{j} , \bar{k} mirrors be defined by non-unit vectors \bar{p} , \bar{q} , \bar{s} respectively, from the corner (origin of the \bar{i} , \bar{j} , \bar{k} triad). Each of the \bar{p} , \bar{q} , \bar{s} contains only two of the base vectors (\bar{i} , \bar{j} , \bar{k}). If the vector product $\bar{p} \times \bar{c}$ is the negative of $\bar{s} \times \bar{c}$, then \bar{p} and \bar{s} lie in a plane containing \bar{c} , and the perpendicular distances from the tips of \bar{p} and \bar{s} to the line containing \bar{c} are equal. That this is true is shown below:

Let \bar{r}_1 be the unit vector representing the ray after the first reflection, and magnitude a the length of this reflected ray from the contact points on the first and second mirrors. Let \bar{r}_2 be the unit vector representing the ray after the second reflection, and b the length of this reflected ray between the contact points on the second and third mirrors. Then we have two vector equations:

$$\bar{p} = \bar{q} - a\bar{r}_1 \text{ and } \bar{s} = \bar{q} + b\bar{r}_2.$$

Operate on the \bar{p} equation by \bar{R}_i from the right, giving, since \bar{p} has no \bar{i} component,

$$\bar{p} \cdot \bar{R}_i = \bar{p} = \bar{q} \cdot (\bar{I} - 2\bar{i}\bar{i}) - a\bar{r}_1 \cdot (\bar{I} - 2\bar{i}\bar{i}),$$

or

$$\bar{p} = \bar{q} \cdot (\bar{I} - 2\bar{i}\bar{i}) + a\bar{c}.$$

Now operate on the above \bar{s} equation by \bar{R}_k from the right, obtaining, since \bar{s} has no \bar{k} component,

$$\bar{s} \cdot \bar{R}_k = \bar{s} = \bar{q} \cdot (\bar{I} - 2\bar{k}\bar{k}) + b\bar{c}$$

Since \bar{q} has no \bar{j} component, it satisfies

$$\bar{q} \cdot (\bar{I} - 2\bar{k}\bar{k}) = -\bar{q} \cdot (\bar{I} - 2\bar{i}\bar{i}).$$

so

$$\bar{s} = -\bar{q} \cdot (\bar{I} - 2\bar{i}\bar{i}) + b\bar{c}.$$

Using these new representations of \tilde{p} and \tilde{s} , one can see that

$$\tilde{p}x\tilde{c} = -\tilde{s}x\tilde{c}$$

Again, one can permute the order of reflections to show generally that the corner of the reflector, and the points of contact of the first and last reflection of a given ray all lie in a plane which contains the incoming and outgoing rays, and that these points of contact are equidistant from a centerline through the corner and parallel to the incoming ray.

Another feature of the corner reflector easily demonstrated from the reflection operator is that if the mirrors are plane, but their normals are not quite orthogonal to each other, then one incoming beam of parallel light will not be uniformly reflected in the reverse direction. Let these non-orthogonal normals be given by n_1, n_2, n_3 and the corresponding reflection operators be $\bar{R}_1, \bar{R}_2, \bar{R}_3$. Now the product $\bar{R}_1 \cdot \bar{R}_2 \cdot \bar{R}_3$ is not equal to this product with subscript indices permuted, so one could expect an incoming beam of parallel light to be reflected in six slightly different directions. Hence, six image portions would be seen when the mirrors deviate significantly from orthogonality.

DISTRIBUTION LIST

<u>No. of Copies</u>	<u>Organization</u>	<u>No. of Copies</u>	<u>Organization</u>
2	Commander Defense Documentation Center ATTN: DDC-TCA Cameron Station Alexandria, VA 22314	1	Director US Army Air Mobility Research and Development Laboratory Ames Research Center Moffett Field, CA 94035
1	Director Defense Nuclear Agency Washington, DC 20305	2	Commander US Army Electronics Command ATTN: AMSEL-RD AMSEL-CE Fort Monmouth, NJ 07703
2	Commander US Army Materiel Command ATTN: AMCMDA, Mr. N. Klein Mr. J. Bender 5001 Eisenhower Avenue Alexandria, VA 22333	2	Commander US Army Missile Command ATTN: AMSMI-R AMSMI-RBL Redstone Arsenal, AL 35809
1	Commander US Army Materiel Command ATTN: AMCRD, BG H.A. Griffith 5001 Eisenhower Avenue Alexandria, VA 22333	5	Commander US Army Missile Command ATTN: AMSMI-RDK Mr. R. Becht (4 cys) Mr. R. Deep Redstone Arsenal, AL 35809
1	Commander US Army Materiel Command ATTN: AMCRD-T 5001 Eisenhower Avenue Alexandria, VA 22333	1	Commander US Army Tank Automotive Command ATTN: AMSTA-RHFL Warren, MI 48090
1	Commander US Army Materiel Command ATTN: AMCRD-W 5001 Eisenhower Avenue Alexandria, VA 22333	2	Commander US Army Mobility Equipment Research & Development Center ATTN: Tech Docu Cen, Bldg. 315 AMSME-RZT Fort Belvoir, VA 22060
1	Commander US Army Aviation Systems Command ATTN: AMSAV-E 12th and Spruce Streets St. Louis, MO 63166	2	Commander US Army Armament Command ATTN: Technical Library Rodman Laboratories Rock Island, IL 61202

DISTRIBUTION LIST

<u>No. of Copies</u>	<u>Organization</u>	<u>No. of Copies</u>	<u>Organization</u>
6	Commander US Army Frankford Arsenal ATTN: Mr. T. Boldt SARFA-U2100 Mr. J. Mitchell SARFA-U3100, S. Fulton SARFA-U3300 Mr. S. Hirshman Mr. A. Cianciosi L4100-150-2 Mr. C. Sleischer, Jr. Philadelphia, PA 19137	1	Commander US Army Research Office ATTN: CRD-AA-EH P. O. Box 12211 Research Triangle Park, NC 27709
7	Commander US Army Picatinny Arsenal ATTN: SARPA-DR-D, S. Wasserman SARPA-DR-V, Mr. A. Loeb Mr. D. Mertz SARPA-V, E. Walbrecht Mr. S. Verner SARPA-VE, Dr. Kaufman Mr. E. Friedman Dover, NJ 07801	1	Director US Army Advanced BMD Technology Center P. O. Box 1500 Huntsville, AL 35809
1	Commander US Army Watervliet Arsenal Watervliet, NY 12189	1	Commander US Army Ballistic Missile Defense Systems Command Huntsville, AL 35804
2	Commander US Army Harry Diamond Labs ATTN: AMXDO-TI H. Davis, Branch 42C Washington, DC 20438	3	Commander US Naval Air Systems Command ATTN: AIR-604 Washington, DC 20360
1	Commander US Army Materials and Mechanics Research Center ATTN: AMXMR-ATL Watertown, MA 02172	3	Commander US Naval Ordnance Systems Command ATTN: ORD-9132 Washington, DC 20360
1	Commander US Army Natick Laboratories ATTN: AMXRE, Dr. D. Sieling Natick, MA 01762	2	Commander and Director US Naval Ship Research and Development Center ATTN: Tech Lib Aerodynamic Lab Washington, DC 20007
		3	Commander US Naval Surface Weapons Center ATTN: Code GX, Dr. W. Kemper Mr. F. H. Maille Dr. G. Moore Dahlgren, VA 22448

DISTRIBUTION LIST

<u>No. of</u> <u>Copies</u>	<u>Organization</u>	<u>No. of</u> <u>Copies</u>	<u>Organization</u>
4	Commander US Naval Surface Weapons Center ATTN: Code 031, Dr. K. Lobb Code 312, Mr. R. Regan Mr. S. Hastings Code 730, Tech Lib Silver Spring, MD 20910	1	AFWL (DEV) Kirtland AFB, NM 87117
		1	ARD (ARIL) Wright-Patterson AFB, OH 45433
		1	ARL Wright-Patterson AFB, OH 45433
3	Commander US Naval Weapons Center ATTN: Code 553, Tech Lib Code 6003, Dr. W. Haseltine Code 511, Mr. A. Rice China Lake, CA 93555	1	ASD (ASBEE) Wright-Patterson AFB, OH 45433
		1	Director National Bureau of Standards ATTN: Tech Lib US Department of Commerce Washington, DC 20234
3	Director US Naval Research Laboratory ATTN: Tech Info Div Code 770C, D. A. Kolb Code 7720, Dr. E. McClean Washington, DC 20390	1	Director NASA Scientific and Technical Information Facility ATTN: SAK/DL P. O. Box 33 College Park, MD 20740
1	Commander US Naval Ordnance Station ATTN: Code FS13A, P. Sewell Indian Head, MD 20640	1	Director Jet Propulsion Laboratory ATTN: Tech Lib 4800 Oak Grove Drive Pasadena, CA 91103
2	ADTC (ADBPS-12) Eglin AFB, FL 32542		
1	AFATL (DLR) Eglin AFB, FL 32542	2	Director National Aeronautics and Space Administration George C. Marshall Space Flight Center ATTN: MS-I, Lib R-AERO-AE, Mr. A. Felix Huntsville, AL 35812
1	AFATL (DLRD) Eglin AFB, FL 32542		
1	AFATL (DLRV) Eglin AFB, FL 32542		
2	AFATL (DLRA, F. Burgess; Tech Lib) Eglin AFB, FL 32542		

DISTRIBUTION LIST

<u>No. of Copies</u>	<u>Organization</u>	<u>No. of Copies</u>	<u>Organization</u>
1	Director National Aeronautics and Space Administration Langley Research Center ATTN: MS 185, Tech Lib Langley Station Hampton, VA 23365	1	Winchester-Western Division Olin Corporation ATTN: Mr. D. Merrill New Haven, CT 06504
1	Director National Aeronautics and Space Administration Lewis Research Center ATTN: MS 60-3, Tech Lib 21000 Brookpark Road Cleveland, OH 44135	1	Sandia Laboratories ATTN: Aerodynamics Dept Org 5629, R. Maydew P. O. Box 5800 Albuquerque, NM 87115
1	Advanced Technology Labs ATTN: Mr. J. Erdos Merrick & Stewart Avenues Westbury, NY 11590	1	California Institute of Technology Geggenheim Aeronautical Laboratory ATTN: Tech Lib Pasadena, CA 91104
2	ARO, Inc. ATTN: Tech Lib Arnold AFS Tennessee 37389	1	Calspan Corporation ATTN: Mr. G. A. Sterbutzel P. O. Box 235 Buffalo, NY 14221
1	Technical Director Colt Firearms Corporation 150 Huyshore Avenue Hartford, CT 14061	2	Franklin Institute ATTN: Dr. Carfagno Dr. Wachtell Race & 20th Streets Philadelphia, PA 19105
1	General Electric Corporation Armaments Division ATTN: Mr. R. Whyte Lakeside Avenue Burlington, VT 05401	1	Director Applied Physics Laboratory The Johns Hopkins University 8621 Georgia Avenue Silver Spring, MD 20910
1	Northrop Corporation Aircraft Division ATTN: Dr. A. Wortman 3901 W. Broadway Hawthorne, CA 92050	1	Massachusetts Institute of Technology Department of Aeronautics and Astronautics ATTN: Tech Lib 77 Massachusetts Avenue Cambridge, MA 02139

DISTRIBUTION LIST

<u>No. of Copies</u>	<u>Organization</u>
1	Ohio State University Department of Aeronautics and Astronautical Engineering ATTN: Tech Lib Columbus, OH 43210
2	Polytechnic Institute of Brooklyn Graduate Center ATTN: Dr. G. Morretti Dr. R. Cresci Farmingdale, NY 11735
1	Princeton University Forrestal Research Center Princeton, NJ 08540
1	Princeton University Forrestal Laboratories ATTN: Dr. S. I. Cheng Princeton, NJ 08540
1	Southwest Research Institute ATTN: Mr. Peter S. Westine P. O. Drawer 28510 8500 Culebra Road San Antonio, TX 78228
2	University of Michigan Department of Aeronautical Engineering ATTN: Dr. A. Kuetcher Dr. M. Sichel East Engineering Building Ann Arbor, MI 48104

Aberdeen Proving Ground

Marine Corps Ln Ofc
Cdr, USATECOM
ATTN: AMSTE-BE
Mr. Morrow
AMSTE-TA-R
Mr. Wise
Dir, USAMSAA